Biointerface Laboratory at Helmholtz-Institute for Biomedical Engineering

RWTH AACHEN UNIVERSITY

Faculty of Medicine

Cell-Material Interactions: Translating Basic Science Into Clinical Applications

Director

Univ.-Prof. Dr. rer. nat.
Wilhelm Jahnen-Dechent

RWTH Aachen University Hospital
Pauwelsstrasse 30, 52074 Aachen

Helmholtz-Institute for Biomedical Engineering
Pauwelsstrasse 20, 52074 Aachen

Phone: +49 (0)241 80-80157 (Secretary)
+49 (0)241 80-80163 (Office)
Fax: +49 (0)241 80-82573
Email: rsous@ukaachen.de
Web: http://www.biointerface.rwth-aachen.de

Staff

Sous, Renate Administrative Assistant
Babler, Anne Dr. rer. nat.
Bienert, Michaela MSc
Biermann, Robin
Bruhns, Florian
Brylka, Laura Dr. rer. nat.
Büscher, Andrea MSc
Carvalho Lopes Barros Menezes, Clara MSc
Dietzel, Eileen Dr. rer. nat.
Floehr, Julia Dr. rer. nat.
Gräber, Steffen CTA
Köppert, Sina Ing. MSc
Labude, Norina MTA
Müller, Katrin MSc
Neuß-Stein, Sabine PD Dr. rer. nat.
Olschok, Kathrin BSc
Peglow, Sarah
Reinhold, Stefan BSc
Schleypen, Tessa BSc
Schmitz, Carlo MSc
Schwarz, Miriam cand med
Weis, Daniel Dr.
Wölfel, Eva Maria MSc
Wosnitza, Elisabeth BSc

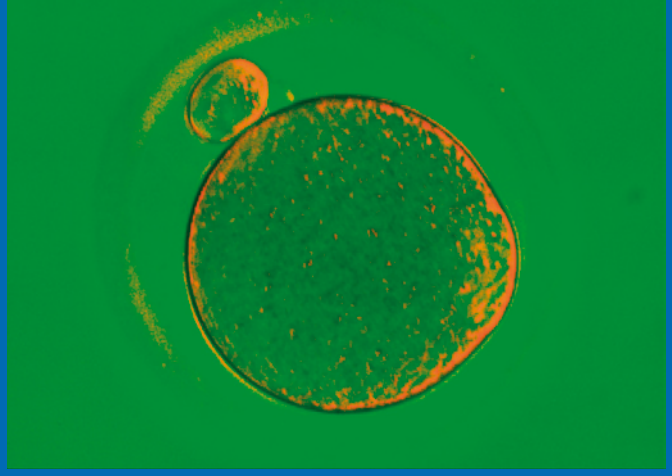

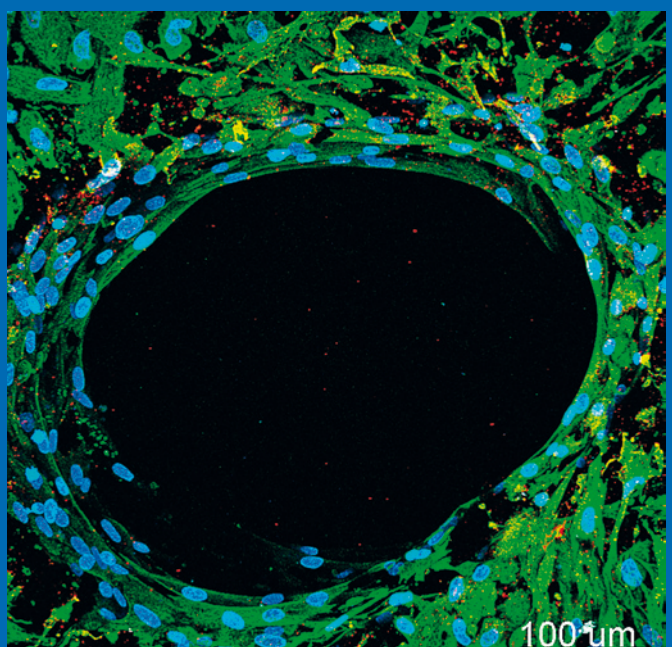

Introduction

This year marks the completion of Julia Floehr's and Laura Brylka's PhD work. They both earned their degrees with distinction. Congratulations! Enjoy their contributions to this report. Kathrin Olschok finished her Bachelor Thesis, Andrea Büscher, Sina Köppert, Eva Wölfel, and Clara Carvalho (Univ. Minho, Portugal) finished their Master Theses. Andrea and Sina continue their work with a PhD thesis, and will report in due course. At the end of the year, Eileen Dietzel moved with her family to the Karolinska Institute in Stockholm, Sweden to spend a post-Doc. We wish her well and many happy returns. Student teaching, graduate training, paper and grant writing is what keeps us busy throughout the year. We secured a training grant that will fund altogether 15 PhD students at University Hospital Aachen, University of Maastricht, The Netherlands, and at the Karolinska Institute, Stockholm, Sweden. Willi Jahnen-Dechent is local coordinator of the Marie Skłodowska Curie training grant IntriCARE that is funded under the Horizon 2020 program. Surely, we will all benefit from this training network. Let us start with a short update on a fruitful area of our lab, fertility research.

Fetuin-B Increases Artificial Fertilization Rate and Is a Target for Contraception

MSc Carlo Schmitz, Dr. Julia Floehr, Dr. Eileen Dietzel



Fetuin-B is a liver-derived serum protein, which diffuses freely from the blood into ovarian follicles[8]. Thus during the development of mammalian oocytes and after fertilization in the oviduct, Fetuin-B is present close to the oocyte. Fetuin-B is an inhibitor of the proteinase ovastacin rendering the *zona pellucida* (ZP), a layer of extracellular matrix surrounding the oocyte, in a hardened state due to proteolytic cleavage of ZP glycoproteins[6]. As a potent inhibitor of ovastacin Fetuin-B prevents premature ZP hardening before fertilization. Thus Fetuin-B keeps the ZP penetrable for sperm until fertilization and maintains female fertility. After fertilization the proteinase ovastacin mediates definitive ZP hardening. It prevents further sperm attachment and penetration, and protects the pre-implantation embryo.

To study Fetuin-B/ovastacin interaction *in vivo*, we generated mice that were deficient for both proteins[3]. While Fetuin-B single deficient female mice (*Fetub*$^{-/-}$) were infertile, due to premature ZP hardening, additional ovastacin deficiency (*Astl*$^{-/-}$) restored fertility (Fig. 1). *Fetub*$^{-/-}$, *Astl*$^{-/-}$ double deficient female mice were fertile. *Fetub*$^{-/-}$, *Astl*$^{-/-}$ females produced offspring, confirming ovastacin proteinase as a prime molecular target of Fetuin-B. Thus, in the absence of the target proteinase ovastacin, the lack of the regulating inhibitor is of no further consequence. The recovery of fertility in *Fetub*$^{-/-}$, *Astl*$^{-/-}$ females underscored the decisive role of Fetuin-B in fertilization, rendering Fetuin-B a potential target for contraception.

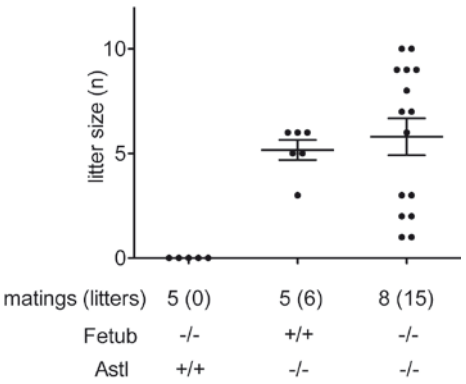

Fig. 1: Fetuin-B / ovastacin double deficiency restores fertility of fetuin B deficient female mice. *Mating study shows that Fetuin-B deficient females (Fetub−/−, Astl+/+) were infertile. Double deficient (Fetub−/−, Astl−/−) females had litters in a comparable size to ovastacin single deficient (Fetub+/+, Astl−/−) females.*

Classical hormone-mediated contraception has intrinsic disadvantages despite proven success and worldwide application in human and animal medicine. Nevertheless, there is an urgent need for contraception to reduce the high number of unintended pregnancies noted in the USA (50%) and worldwide (40%). Contraception should prevent pregnancies, be reversible and well tolerated. Considering these requirements, we studied if Fetuin-B down-regulation could be used for non-hormonal contraception. To achieve this, we analyzed the fertility of female mice undergoing Fetuin-B down-regulation by antisense oligonucleotide treatment. The immunoblot in figure 2A illustrates a typical serum Fetuin-B down-regulation within 50 days and the following washout period during the recovery

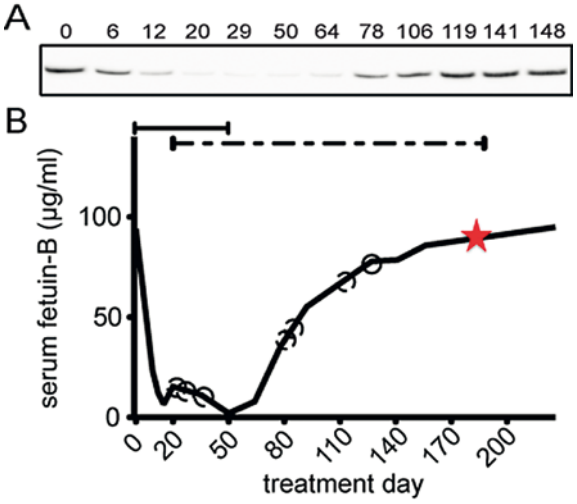

Fig. 2: Fetuin-B* antisense oligonucleotide-*mediated down-regulation of serum Fetuin-B causes infertility. *(A) Representative mouse Fetuin-B immunoblot shows serum Fetuin-B level during (day 0–50) and after the antisense oligonucleotide treatment. (B) Serum Fetuin-B decreased during antisense oligonucleotide treatment (continuous line). Mating (dashed line) was from day 20 onwards. Black circle indicates vaginal plug without pregnancy. Red star symbolizes a vaginal plug followed by pregnancy.*

time course. Upon mating the Fetuin-B antisense oligonucleotide-treated females (11/12) did not become pregnant while PBS-treated females (10/10) had litters. Furthermore, the antisense oligonucleotide treatment was reversible. When the antisense treatment was stopped and serum Fetuin-B returned to the base level, females became pregnant. Consequently, we showed that pharmacological Fetuin-B down-regulation by antisense oligonucleotide therapy results in reversible infertility in female mice and can be used for contraception.

Besides the usefulness of ZP hardening for contraception, it is also a common complication in assisted reproductive medicine. To keep the ZP unhardened and penetrable, it is common practice to use serum-derived factors as media supplements. Common additives include fetal calf serum, bovine fetuin and human serum or human follicular fluid, all of which contain Fetuin-B. Lot-to-lot variation, in for example human serum and human serum albumin, has been blamed for low pregnancy rates following assisted reproductive techniques. Strict quality control must ensure that media are free of infectious proteins and viruses. Thus, we studied the addition of recombinant Fetuin-B protein instead of sera to inhibit premature ZP hardening and to obtain defined media[4]. Figure 3A shows that when sperm were added to oocytes immediately after isolation (0 hours of *in vitro* culture), embryos developed to the two-cell stage in comparable numbers regardless of supplementation of the IVF medium with recombinant mouse Fetuin-B. However, when *in vitro* culture was increased for up to one or five hours, addition of recombinant mouse Fetuin-B to the IVF medium increased the IVF
rate. Two-cell embryos (Fig. 3B, E) de veloped into four-cell embryos (Fig. 3C, F) and further into blastocysts (Fig. 3D, G). Embryos that were fertilized in recombinant mouse Fetuin-B containing medium had larger numbers of sperm attached to them, suggesting that recombinant mouse Fetuin-B inhibited fertilization-triggered ZP hardening, which normally prevents further sperm attachment. Thus recombinant mouse Fetuin-B inhibited ZP hardening as expected but did not increase embryo loss despite multiple sperm binding.

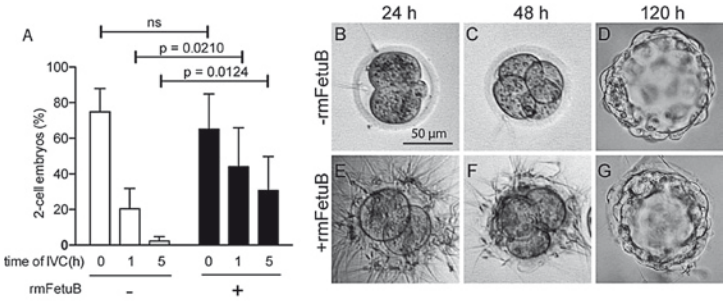

Figure 3: Recombinant mouse Fetuin-B (rmFetuB) increases in vitro fertilization (IVF) rate for up to five hours of in vitro culture (IVC). *(A) IVF was performed in medium without rmFetuB (white columns) or in medium containing 0.05 mg/ml rmFetuB (black columns). Embryos developed normally without (B-D) or with added rmfetuB (E-G) according to developmental stage at 24 hours post fertilization (B, E), 48 hours (C, F) and 120 hours (D, G). All micrographs were taken using the same magnification.*

The Role of Fetuin-A in Endochondral Ossification

Dr. Laura Brylka

Using genetically engineered mouse models, we established that the main function of the hepatic plasma glycoprotein Fetuin-A is to inhibit ectopic calcification. Fetuin-A deficient mice (*Ahsg*$^{-/-}$) on the calcification-sensitive genetic background DBA/2 develop extensive soft tissue calcification in almost all major organs. In patients suffering from chronic kidney disease, which leads to extensive vascular calcification, high Fetuin-A levels correlate with increased survival rates. Through its capacity to bind calcium phosphate mineral, Fetuin-A facilitates the clearance of excess mineral from the body. As mineralized bone tissue contains huge amounts of calcium phosphate, it is not surprising, that Fetuin-A accumulates in bone in high abundance. Fetuin-A is indeed one of the most highly abundant non-collagenous proteins in bone. Fetuin-A deficient mice on the genetic background C57BL/6 and to a lesser extent also on DBA/2 background develop a bone phenotype anomaly. In adult mice, the femoral bones are shorter and their growth plates are disordered, while all the other bones are normal in size.
Long bones develop through endochondral ossification. This process starts with the aggregation of mesenchymal stem cells and their differentiation into chondrocytes. The resulting cartilaginous bone template increases in size and is gradually replaced by bone through continuous proliferation, cell maturation, and vascular invasion. In order for the bone to grow in length, cartilaginous regions remain at opposite ends of the long bone, the so-called growth plates. These growth plates contain chondrocytes of different maturation stages arranged in distinct zones. In the reserve zone, immature chondrocytes serve as a reservoir. Then, chondrocytes start to proliferate, forming neatly ordered stacks of cells.

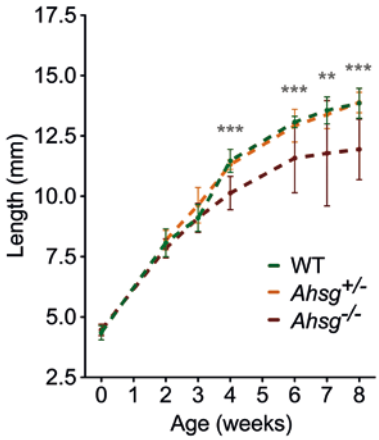

Fig. 4: The development of femur length over time. *While femur growth was similar in wildtype and Fetuin-A heterozygous mice, femur length was significantly decreased in Ahsg*$^{-/-}$ *mice, starting from four weeks of age.*

Subsequently, the chondrocytes become hypertrophic. Late hypertrophic chondrocytes mineralize their matrix. Finally, the chondrocytes either differentiate into osteoblasts or they undergo apoptosis. The calcified cartilage is replaced by bone. Continuous proliferation and differentiation of growth plate chondrocytes and subsequent remodeling of the growth plate cartilage lead to an elongation of the bone.

To investigate the bone phenotype anomaly in Fetuin-A deficient mice, and thus the role of Fetuin-A in longitudinal bone growth, we studied the development of the femur in wildtype, heterozygous (*Ahsg*$^{+/-}$) and homozygous Fetuin-A deficient (*Ahsg*$^{-/-}$) mice, starting from newborn mice until eight weeks of age. While femur growth was similar in wildtype and *Ahsg*$^{+/-}$ mice, femur length was significantly decreased in Fetuin-A deficient *Ahsg*$^{-/-}$ mice, starting from four weeks of age (Fig.4). To better understand the morphological changes in femora from *Ahsg*$^{-/-}$ mice, femora from eight weeks old mice were measured using micro-computed tomography (μCT) (Fig. 5). Femora from *Ahsg*$^{-/-}$ mice were notably bent in their distal region. Also, their growth plates were angularly deformed (Fig. 5F). Taken together these results suggest that at the age of four weeks the distal femur had started to deform.

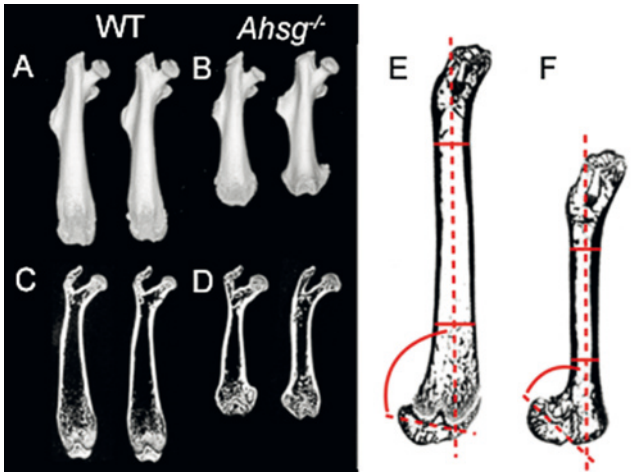

***Fig. 5: Micro-computed tomography (µCT) reveals morphological features in femora from eight weeks old Fetuin-A deficient mice**. Three-dimensional reconstructions of bones from wildtype (A) and Ahsg$^{-/-}$ mice (B) and the respective two-dimensional cross-sections (C, D) show morphological changes in Ahsg$^{-/-}$ femora. The growth plates from Ahsg$^{-/-}$ bones (F) were deformed in such a way that the angle of the growth plate with respect to the shaft was decreased (E).*

In order to understand the development of the bone dysplasia in *Ahsg*$^{-/-}$ mice, we studied histological sections from mice of different ages. Starting from newborn mice, until about three weeks of age, the zone of hypertrophic chondrocytes was elongated (Fig. 6). At three weeks of age, the elongated hypertrophic zone disappeared. At this time point cellular infiltrates localized in growth plates between the proliferative and hypertrophic zone. These infiltrates were not only found in *Ahsg*$^{-/-}$ mice, but also in heterozygous *Ahsg*$^{-/-}$ mice. To investigate the underlying mechanisms leading to cellular infiltration and growth plate deformation, we performed a microarray analysis on growth plate cartilage in collaboration with the Genomics Facility of the IZKF Aachen. Using laser capture microdissection of frozen bone section, we isolated whole growth plates from 13 days old wildtype, *Ahsg*$^{+/-}$ and *Ahsg*$^{-/-}$ mice. RNA was extracted from the isolated growth plate cartilage and used for microarray analysis. Gene enrichment analysis showed that in the growth plates of *Ahsg*$^{-/-}$ mice, genes involved in the regulation of the immune response were highly overexpressed. The most highly upregulated genes were mainly regulated by interferon signaling, as shown by a comparison of the data to the interferome database. The single most highly upregulated gene, with an upregulation of about 560-fold, was the chemokine CXCL9. This chemokine is predominantly expressed during inflammation and it recruits effector T cells to the site of inflammation. The high upregulation of CXCL9 in the growth plates of *Ahsg*$^{-/-}$ mice points to a specific inflammatory mechanism.

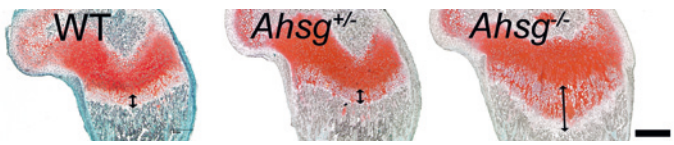

***Fig. 6: Elongated hypertrophic zones in bones from 13 days old Ahsg$^{-/-}$ mice.** Histological femur sections were stained with safranin O and fast green FCF. The two-sided arrow marks the length of the hypertrophic zone, which was severely elongated in Ahsg$^{-/-}$ mice. Scale bar is 200 µm.*

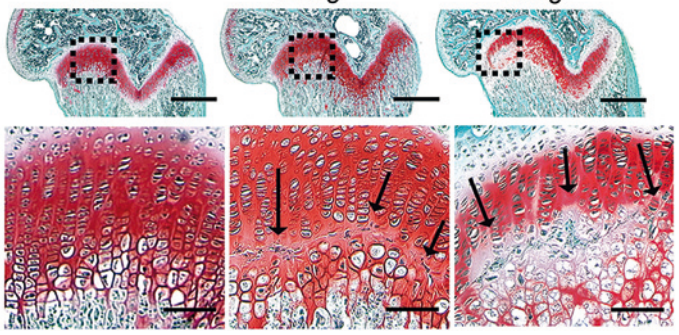

***Fig. 7: Cellular infiltrates in the growth plates of three weeks old Fetuin-A deficient mice.** Histological femur sections stained with safranin O and fast green FCF show the presence of cellular infiltrate located between the proliferative and the hypertrophic zone (arrows) in the growth plates of both, Ahsg$^{+/-}$ and Ahsg$^{-/-}$ mice. Scale bars upper panels are 200 µm, lower panels 50 µm.*

Taken together, our results suggest an anti-inflammatory role for Fetuin-A in endochondral ossification. We will further investigate the mechanisms leading to the inflammatory response in the growth plates of Fetuin-A deficient mice. This will deepen our understanding not only of fetuin biology, but also of growth plate physiology and pathology.

Stem Cells and Tissue Engineering

PD Dr. Sabine Neuß-Stein

In 2016 members of the group „Stem Cells and Tissue Engineering“ published data gained in long-lasting cooperations with clinicians and basic scientists. Together with Bernd Lethaus from the Department of Oral and Maxillofacial Surgery, tissue engineered bone constructs were proved to be functional for the first time in a large animal model. Therefore, ovine

MSC (oMSC) were isolated, expanded and characterized before they seeding on 3D Poly-D-L-Lactid acid (PDLLA), Poly-Ether-Keton-Keton (PEKK) and silk (± hydroxyapatite (HA)) scaffolds. The tissue engineered constructs were autologously transplanted in critical size defects in an ovine calvarial model for three months. Histological stainings and microradiographic analyses identified PEKK scaffolds as suitable biomaterial for bone tissue engineering (Fig. 8).

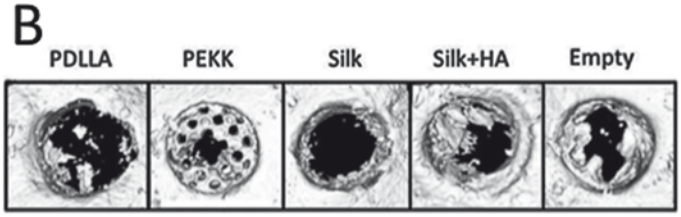

Fig. 8: Tissue engineered bone constructs seeded with autologous ovine mesenchymal stem cells. *A) Critical size defects in a calvarial sheep model were filled with in vitro derived bone constructs for three month. B) Microradiographic analysis demonstrates highest amounts of newly formed bone in PEKK transplants.*

Besides advancing bone tissue engineering strategies from cell culture to large animal models, the group used the biomaterial test platform – established in 2007 – to unravel further biomaterials suitable for bone tissue engineering in combination with human dental pulp stem cells (DPSC). This work was done in cooperation with Christian Apel (Department of Tissue Engineering and Textile Implants). Here, DPSC were seeded on 17 different polymers for 21 days either in osteogenic induction medium or in stem cell expansion medium followed by RealTime PCR of osteogenic marker genes, Alizarin red staining and analysis of alkaline phosphatase secretion. Surprisingly, on the molecular level, alginate, hyaluronic acid and Polyvinylidenfluoride (PVDF) initiated osteogenic differentiation of DPSC without addition of induction factors.
Together with Andrij Pich (DWI) and Georg Conrads (Oral Microbiology and Immunology) the group was successful in developing Isoeugenol-based nanogels for implant coatings repelling microorganisms – here antibacterial activity against oral pathogens was demonstrated - and in parallel exhibiting cell adhesive properties. Such functional nanogels can be used to design implant coatings preventing biofilm formation during tissue regeneration and wound healing processes. (Fig.9).

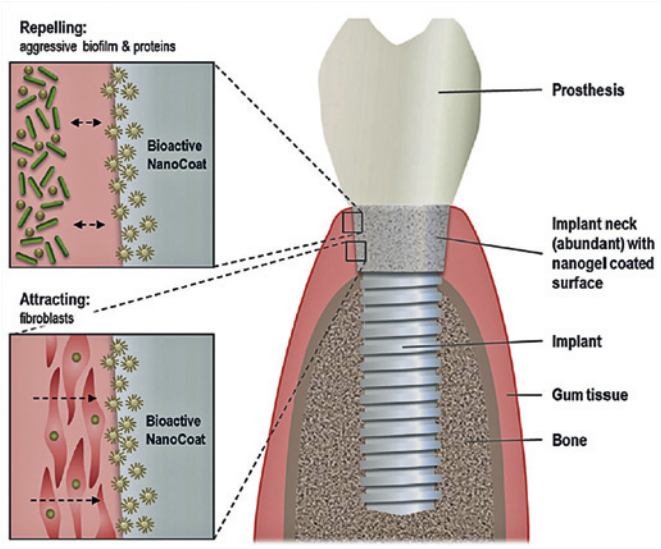

Fig. 9: Concept of bioactive nanogel coatings for (dental) implants. *Kather* et al., *Angew Chem Int Ed, 2016.*

Increasing Biocompatibility of Patient-Specific PEO-Coated Implants Using Endothelial Progenitor Cells and Mesenchymal Stem Cells in Bone Defects

MSc Michaela Bienert

Bone graft vascularization is a main challenge in tissue engineering to improve biocompatibility. Osseointegration and reconstruction of function after implantation can be achieved by support of a bone environment rich in vascular networks. In our study, structural and vascular integration was achieved by using plasma electrolytic oxidation (PEO)-coated magnesium grafts cultured with autologous mesenchymal stem cells (MSC) and endothelial progenitor cells (EPC) from peripheral blood. Magnesium grafts were designed in a patient-specific way using selective laser melting (SLM) data from the Fraunhofer ILT Aachen. Materials were bated before PEO-coating and coated grafts were compared to non-coated grafts. To enable EPC and MSC culture, graft materials needed to be sterile before they were used in cell culture. In figure 10 four different prevalent sterilization methods were shown.
Color changes in the implants could be observed when materials were autoclaved or treated with EtOH. No color changes could be observed when implants were heated or exposed to UV-C light. Compared to the other methods UV-C provided a gentle method for sterilization. For further studies materials are sterilized using UV-C light.
For cytotoxicity studies of magnesium grafts with or without PEO-coating, grafts were incubated for 24 h in cell culture media. Human vein endothelial cells (HUVEC) or human MSC were seeded on cell culture plastic. Media

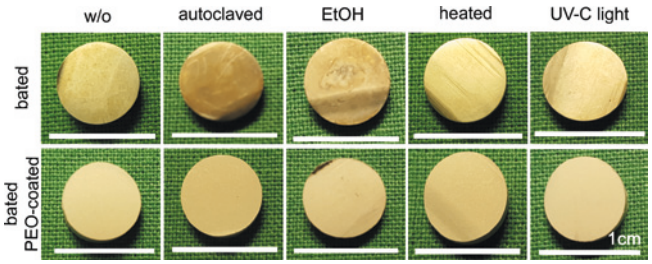

Fig. 10: Comparison of different sterilization methods for bated magnesium implants with and without PEO-coating. *Bated implants or bated PEO-coated implants were either autoclaved for 120 min at 121 °C and 2.12 bar, washed for 5 min in 70 % EtOH followed by washing in PBS for 5 min, heated for 3 h at 160 °C or exposed to UV-C light for 25 min and compared to non-treated materials (w/o). Scale bar indicates 1 cm.*

incubated with grafts were added to respective cells and incubated for 24 h. Afterwards cells were stained with fluorescein diacetate (FDA) and propidium iodide (PI). Figure 11 shows fluorescence microscopy pictures of live/dead staining of the respective materials with viable cells in green and dead cells in red.

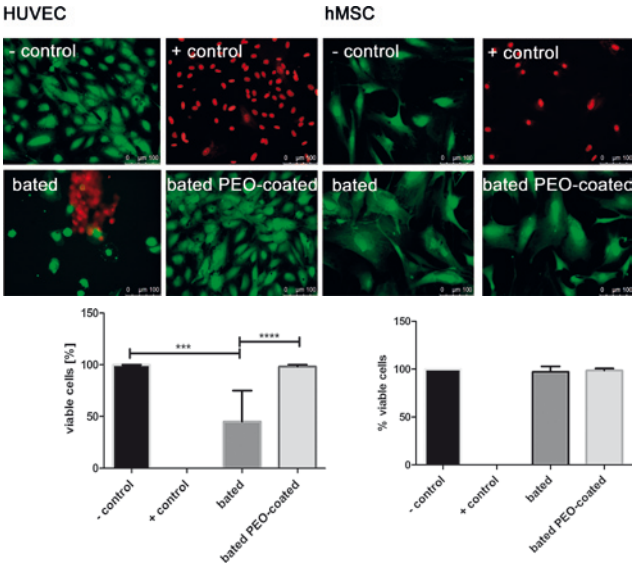

Fig. 11: Cytotoxic effects of magnesium grafts coated with or without polyethylene oxide (PEO). *Grafts with or without PEO-coating were incubated for 24 h in cell culture media. Subsequently HUVEC or hMSC were incubated with this media for 24 h. Afterwards live/dead staining occurred using FDA (green/viable cells) and PI (red/dead cells). Quantification performed using, t-test, CI 95 %, p***= 0.0007 and p****< 0.0001, representative for n=3.*

Bating of the magnesium grafts significantly reduced HUVEC viability compared to negative control and PEO-coated material. This indicates that PEO-coating is essential for HUVEC viability. In contrast PEO-coating is not essential for MSC viability.

Selected References

[1] Jahnen-Dechent W, Brylka L, Schinke T, McKee MD. Letter to the Editor, concerning: "FGF23-regulated production of fetuin-A (AHSG) in osteocytes". Bone 2016;93:223–224.

[2] Pasch A, Block GA, Bachtler M, Smith ER, Jahnen-Dechent W, Arampatzis S, Chertow GM, Parfrey P, Ma X, Floege J. Blood calcification propensity, cardiovascular events and survival in patients receiving hemodialysis in the EVOLVE trial. *Clin J Am Soc Nephrol.* 2016;1–66.

[3] Floehr J, Dietzel E, Schmitz C, Chappell A, Jahnen-Dechent W. Down-regulation of the liver-derived plasma protein fetuin-B mediates reversible female infertility. *Mol Hum Reprod* [Internet]. 2016;gaw068–14.

[4] Dietzel E, Floehr J, Van de Leur E, Weiskirchen R, Jahnen-Dechent W. Recombinant fetuin-B protein maintains high fertilization rate in cumulus cell-free mouse oocytes. *Mol Hum Reprod* [Internet]. 2016;1–12.

[5] van de Kamp J, Paefgen V, Wöltje M, Böbel M, Jaekel J, Rath B, Labude N, Knüchel R, Jahnen-Dechent W, Neuss S. Mesenchymal stem cells can be recruited to wounded tissue via hepatocyte growth factor-loaded biomaterials. *J Tissue Eng Regen Med.* 2016

[6] Dietzel E, Floehr J, Jahnen-Dechent W. The Biological Role of Fetuin-B in Female Reproduction. *Annals of Reproductive Medicine and Treatment.* 2016;1–4.

[7] Bartneck M, Fech V, Ehling J, Govaere O, Warzecha KT, Hittatiya K, Vucur M, Gautheron J, Luedde T, Trautwein C, Lammers T, Roskams T, Jahnen-Dechent W, Tacke F. Histidine-Rich Glycoprotein Promotes Macrophage Activation and Inflammation in Chronic Liver Disease. *Hepatology.* 2016;63:1310–1324.

[8] Floehr J, Dietzel E, Neulen J, Rösing B, Weissenborn U, Jahnen-Dechent W. Association of high fetuin-B concentrations in serum with fertilization rate in IVF: a cross-sectional pilot study. *Hum Reprod.* 2016;31:630–637.

[9] Keyzer CA, De Borst MH, Van den Berg E, Jahnen-Dechent W, Arampatzis S, Farese S, Bergmann IP, Floege J, Navis G, Bakker SJL, Van Goor H, Eisenberger U, Pasch A. Calcification Propensity and Survival among Renal Transplant Recipients. *J Am Soc Nephrol.* 2016;27:239–248.

[10] Kather M., Skischus M., Kandt P., Pich A.,* Conrads G.,* Neuss S.* Functional isoeugenol-modified nanogel coatings for design of biointerfaces. Angew Chem Int Ed, 2016, DOI: 10.1002/anie.201609180R1.

[11] Apel C., Buttler P., Salber J., Dhanasingh A., Neuss S. Differential mineralization of human dental pulp stem cells on different polymers. Biomedizinische Technik / Biomedical Engineering, accepted (Dez. 2016).

[12] Adamzyk C, Labude N, Schneider RK, Jäckel J, Hoffmann V, Fischer J, Hoss M, Knuechel R, Jahnen-Dechent W, Neuss S. Human Umbilical Cord-Derived Mesenchymal Stem Cells Spontaneously Form 3D Aggregates and Differentiate in an Embryoid Body-Like Manner. JSRT. 2016;1:1–9.

[13] Adamzyk C, Kachel P, Hoss M, Gremse F, Modabber A, Hoelzle F, Tolba R, Neuss S, Lethaus B. Bone tissue engineering using polyetherketoneketone scaffolds combined with autologous mesenchymal stem cells in a sheep calvarial defect model. J Craniomaxillofac Surg. 2016;44:985–994.

Team